NOTES AND CORRESPONDENCE

Use of a High-Resolution Model to Analyze the Mapping Capabilities of Multiple-Altimeter Missions

P. Y. LE TRAON, G. DIBARBOURE, AND N. DUCET

Space Oceanography Division, CLS, Ramonville Saint-Agne, France

18 January 2000 and 26 December 2000

ABSTRACT

The contribution of merging multiple-satellite altimeter missions to the mapping of sea level is analyzed from a North Atlantic high-resolution (1/10°) numerical simulation. The model is known to represent the mesoscale variability quite well and offers a unique opportunity for assessing the mapping capability of multiple-altimeter missions. Several existing or planned orbits [TOPEX/Poseidon (T/P), *Jason-1*, *ERS-1/2*–ENVISAT, GEOSAT-GFO] are analyzed, and *Jason-1* and T/P orbits are assumed to be interleaved. The model sea level anomaly fields are first subsampled along T/P, ERS, GFO, and *Jason-1* tracks and a random noise of 3-cm rms is added to the simulated altimeter data. A suboptimal mapping method is then used to reconstruct the 2D sea level anomaly from alongtrack data and the reconstructed fields are compared with the reference model fields. Comparisons are performed in the North Atlantic and over a complete year. These results confirm the main conclusions of the Le Traon and Dibarboure study based on formal error analysis. There is, in particular, a large improvement in mapping capability when going from one to two satellites. Mapping errors (in percentage of the signal variance) are, however, larger than the ones derived from formal error analysis (by a factor between 1.5 and 2) and do not decrease as rapidly. This is mainly due to the high-frequency (periods $<$ 20 days) and high-wavenumber signals of the Los Alamos model, which cannot be resolved with any of the analyzed multiple-satellite configurations.

1. Introduction

The usually agreed main requirement for future altimeter missions is that at least two altimeter missions with one very precise long-term altimeter system are needed (Koblinsky et al. 1992). The long-term altimeter system is supposed to provide the low-frequency and large-scale climatic signals and to provide a reference for the other altimeter missions. It requires a series of very precise and intercalibrated missions. TOPEX/Poseidon (T/P) and later on the Jason series have been designed to meet these objectives. The role of the other missions is to provide the higher wavenumbers and frequencies and, in particular, the mesoscale signal, which cannot be well observed with a single-altimeter mission. This does not require precise altimeter systems as most of the altimetric errors are at long wavelength and they do not impact significantly the mesoscale signal.

Such a requirement for future altimeter missions is partly based on several studies on the sampling characteristics of single- and multiple-altimeter missions (e.g., Wunsch 1989; Chassignet et al. 1992; Blayo et al. 1997; Greenslade et al. 1997; Le Traon and Dibarboure 1999), although these studies do not always provide quantitative and consistent estimations of the merging contribution. Le Traon and Dibarboure (1999, hereafter LD99) have analyzed, in particular, the mesoscale mapping capabilities of multiple-altimeter missions. They used a space–time suboptimal interpolation method to estimate the sea level anomaly (SLA) and velocity formal mapping errors for different orbit configurations. Their main conclusions were that existing and future two-satellite configurations [T/P and European Remote Sensing Satellite (ERS) and later on *Jason-1*, and the European Space Agency's Environment Satellite (ENVISAT)] will provide a rather good mapping of SLA mesoscale variability (SLA mapping error below 10% of the signal variance). These conclusions differ, however, from those of Greenslade et al. (1997, hereafter GCS97), who concluded that the mesoscale variability cannot be mapped with an acceptable accuracy with any of the existing or future two- or three-satellite configurations. GCS97 required, however, a very homogenous mapping error. Although the mesoscale mapping errors

Corresponding author address: Dr. P. Y. Le Traon, Head Oceanography Dept., Space Oceanography Division, CLS, 8–10 rue Hermes Parc Technologique du Canal, Ramonville Saint-Agne Cedex 31526, France.
E-mail: letraon@cls.fr

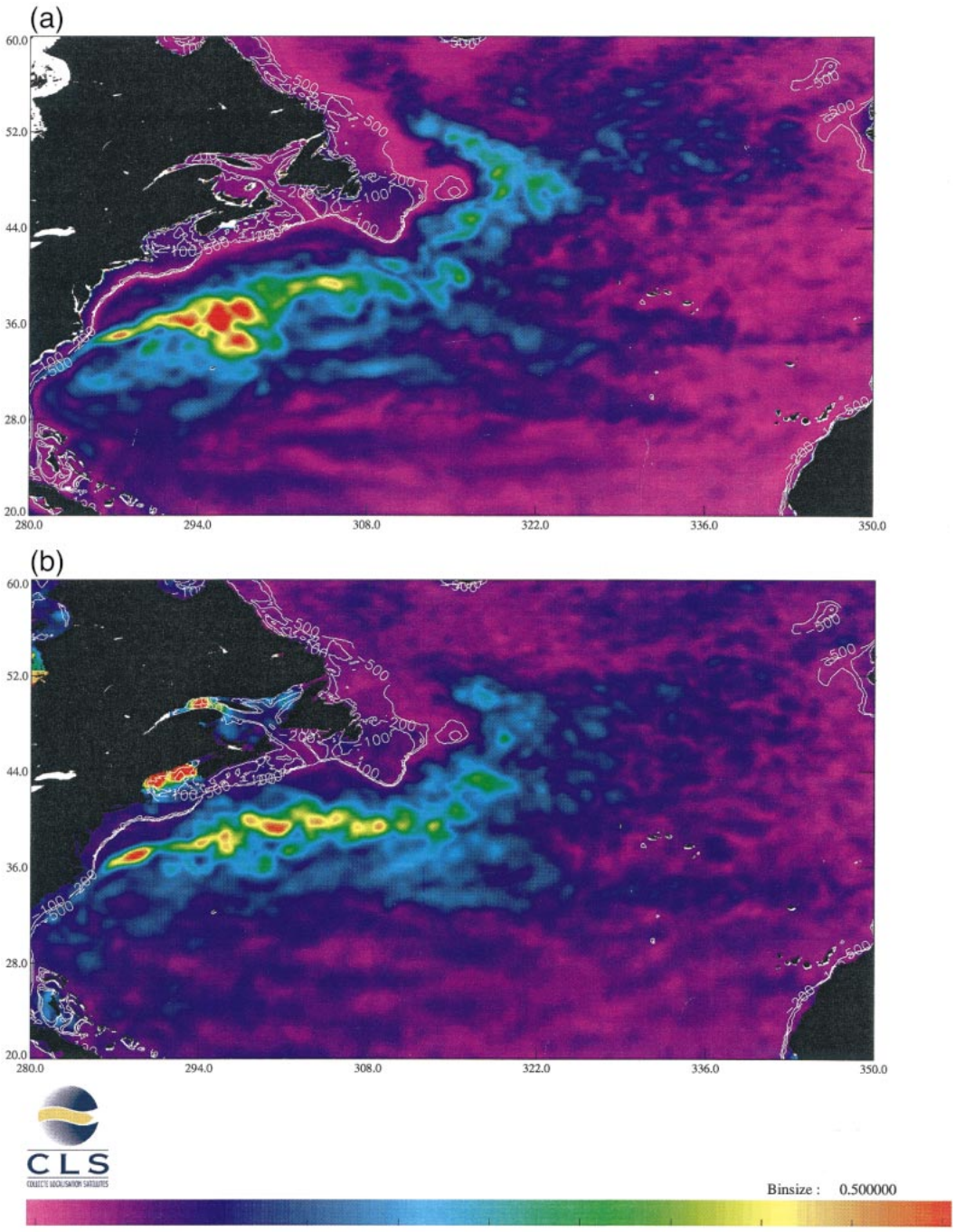

FIG. 1. (a) LAM (Smith et al. 2000) rms sea level variability for year 1993. (b) Rms sea level variability for year 1993 from the combination of T/P and *ERS-1* data (Ducet et al. 2000).

are not homogenous, LD99 argue that they remain sufficiently small relative to the signal.

The mapping capability of single- and multiple-altimeter missions is thus still an open and important issue. This paper provides an extension of an LD99 study using the Los Alamos North Atlantic model simulation (hereafter LAM) (Smith et al. 2000). The LAM is a 1/10° primitive equation model forced with realistic winds. It is one of the first basin-scale models with a mesoscale variability in quantitative agreement with T/P and *ERS-1/2* altimeter data (Smith et al. 2000; Ducet 2000) (Figs. 1a,b). The model thus offers a unique opportunity for assessing the mapping capabilities of single- and multiple-altimeter missions. This will allow us to quantify how well the irregular space–time sampling of altimeter missions can map a very complex field of motion where high-

and low-frequency and wavenumber signals are superimposed. Such an analysis is also needed for a better altimeter data interpretation.

As in LD99 (and GCS97), only the mapping capabilities are analyzed, that is, only a priori statistical information (covariance) on the field to be mapped is used. This allows us to quantify the contribution of the data themselves, which is the main objective of our study. This estimation of sampling requirements thus takes no account of models and assimilation that can alter the spatial and temporal requirements. Using information on model dynamics in a data assimilation perspective would be the next logical and complementary step of this study. This is, however, a much more complex issue (especially at these very high resolutions).

This note is organized as follows. Methods are presented in section 2. Section 3 shows some illustrative results, while statistical results are given in section 4. Discussion and main conclusions are found in sections 5 and 6, respectively.

2. Methods

The model sea level outputs were first transformed into sea level anomaly data by removing a 3-yr mean (1993–95). They were then subsampled to obtain simulated alongtrack altimeter datasets for T/P, *Jason-1*, ERS (or ENVISAT), and the Geosat Follow-On (GFO). A random ''altimeter'' noise of 3-cm rms was added to the simulated alongtrack SLA data. As in LD99, we did not take into account long-wavelength errors for the different altimetric missions as these errors could be partly reduced prior to or during the mapping procedure by using the more precise mission (T/P and later on Jason) as a reference (e.g., Le Traon and Ogor 1998; Le Traon et al. 1998).

The simulated datasets were then used to reconstruct the SLA gridded fields using a space–time suboptimal interpolation method. The method is detailed in Ducet et al. (2000). It uses the following space [zero crossing of correlation function (ZC)] and time [*e*-folding time (ET)] correlation scales:

$$\mathrm{ZC} = 50 + 250\left(\frac{900}{\mathrm{lat}^2 + 900}\right) \text{ km},$$

where lat stands for latitude, in degrees, and

$$\mathrm{ET} = 15 \text{ days}.$$

These scales are intended to represent typical time- and space scales of SLA as they can be observed from altimetry (e.g., Stammer 1997). Ducet et al. (2000) used them, in particular, to map sea level and ocean circulation at high resolution from T/P and *ERS-1/2* data. Our covariance functions are thus only approximations of the ''true'' (i.e., here derived from model fields) covariance functions, which is more representative of an actual mapping exercise. Ducet (2000) shows, however, that the Los Alamos model space scales and timescales are close to the scales derived from altimeter data.

The signal mapping (contrary to the formal error estimation) is not very sensitive, in any case, to these a priori choices when the constraint from the data is strong. For example, in the Gulf Stream area, the variance of the actual mapping error (i.e., obtained from the difference between the model fields and the reconstructed fields—see below) for the T/P+Jason-1 configuration varies by only ±10% for different choices of time- and space scales ranging from 100 to 200 km and 10 to 20 days, respectively. Note that our ZC and ET choice at this latitude provides one of the smallest mapping errors. The formal mapping error varies, on the other hand, by a factor of 2–3.

The estimations are performed on a regular 1/10° × 1/10° grid. We chose to analyze the following configurations:

- One altimeter: T/P (or Jason-1), ERS (or ENVISAT), GFO;
- Two altimeters: T/P+ERS, T/P+Jason-1;
- Three altimeters: T/P+ERS+GFO; and
- Four altimeters: T/P+Jason-1+ERS+GFO.

The *Jason-1* and T/P orbits are assumed to be interleaved with no time lag between the two satellites. This is the nominal scenario for the science tandem phase of T/P and *Jason-1*. It can be considered as an optimal sampling design for a two-satellite configuration.

Comparison of the reconstructed fields with the reference model fields (resampled on the regular 1/10° × 1/10° grid) allows an estimation of the mapping error. The main interest of such a simulation is that it allows us to visualize the mapping errors. In practice, the comparison was made over a 1-yr period (1993) with maps calculated every 9 days, that is, we compared a total of 40 maps. The calculations were done on a large area from 20° to 60°N and 80° to 5°W, that is, covering the full North Atlantic.

3. A few illustrative results in the Gulf Stream

As an illustration, Figs. 2a–d show the LAM absolute sea level (i.e., the model 3-yr mean was added to the sea level anomaly) from 20 to 29 January 1993 in an area centered on the Gulf Stream. The LAM signal ranges from −100 cm to +100 cm and corresponds to meanders, rings, or eddies of the Gulf Stream and its extension. The 23 January 1993 field was reconstructed from T/P, T/P+ERS, T/P+ERS+GFO, and T/P+Jason-1+ERS+GFO simulated alongtrack data. The mapping errors, that is, the differences with the reference LAM field (shown on Fig. 2b), are shown on Figs. 3a–d for the different orbit configurations. The signal is qualitatively well recovered with all configurations. Only the T/P case shows large differences with the reference field. The rms differences are 14.4, 10, 7.7, and 7.2 cm for T/P, T/P+ERS, T/P+ERS+GFO, and T/P+Jason-

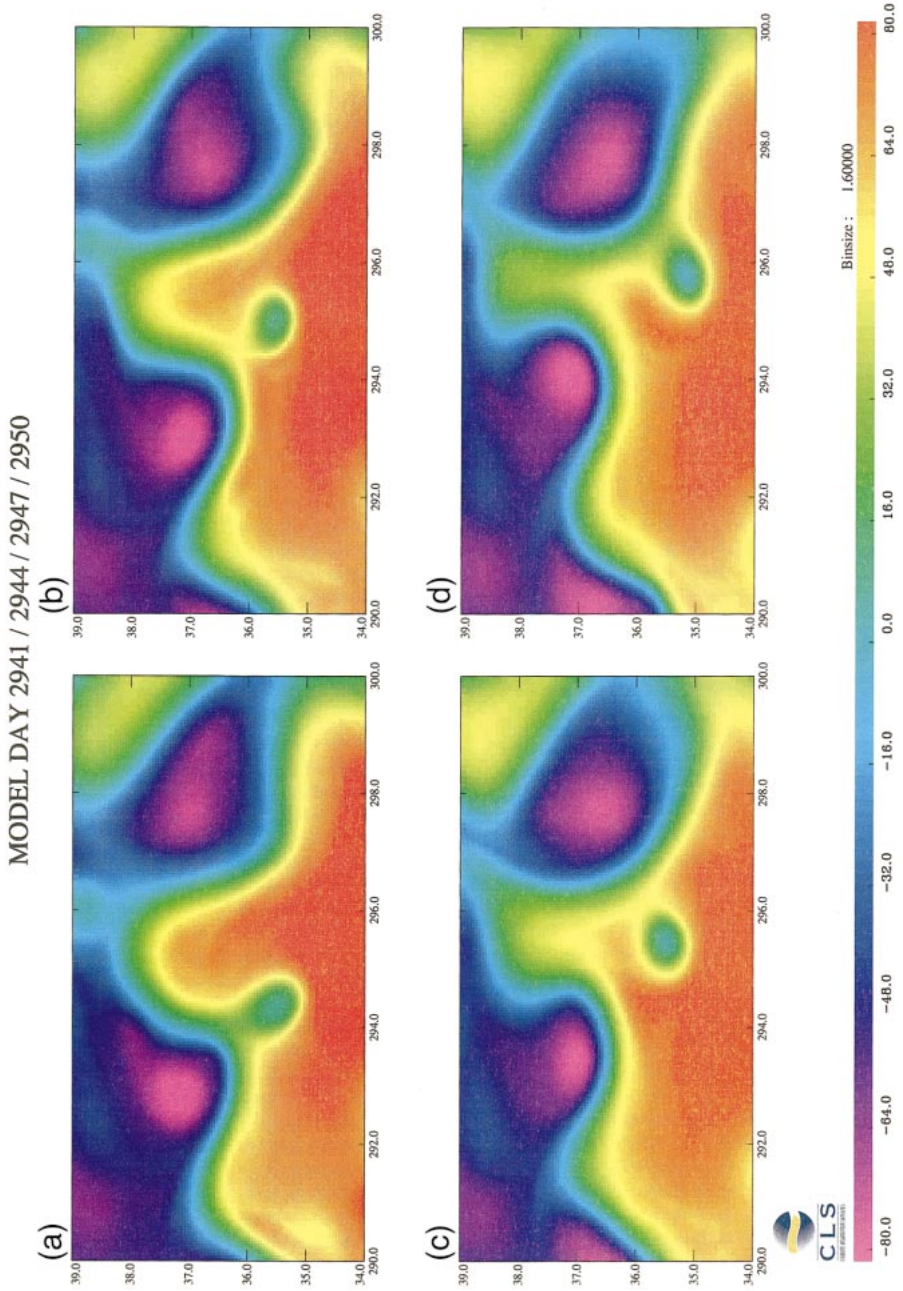

FIG. 2. LAM absolute sea level in the Gulf Stream area for (a) 20 Jan, (b) 23 Jan, (c) 26 Jan, and (d) 29 Jan 1993. Units are in centimeters.

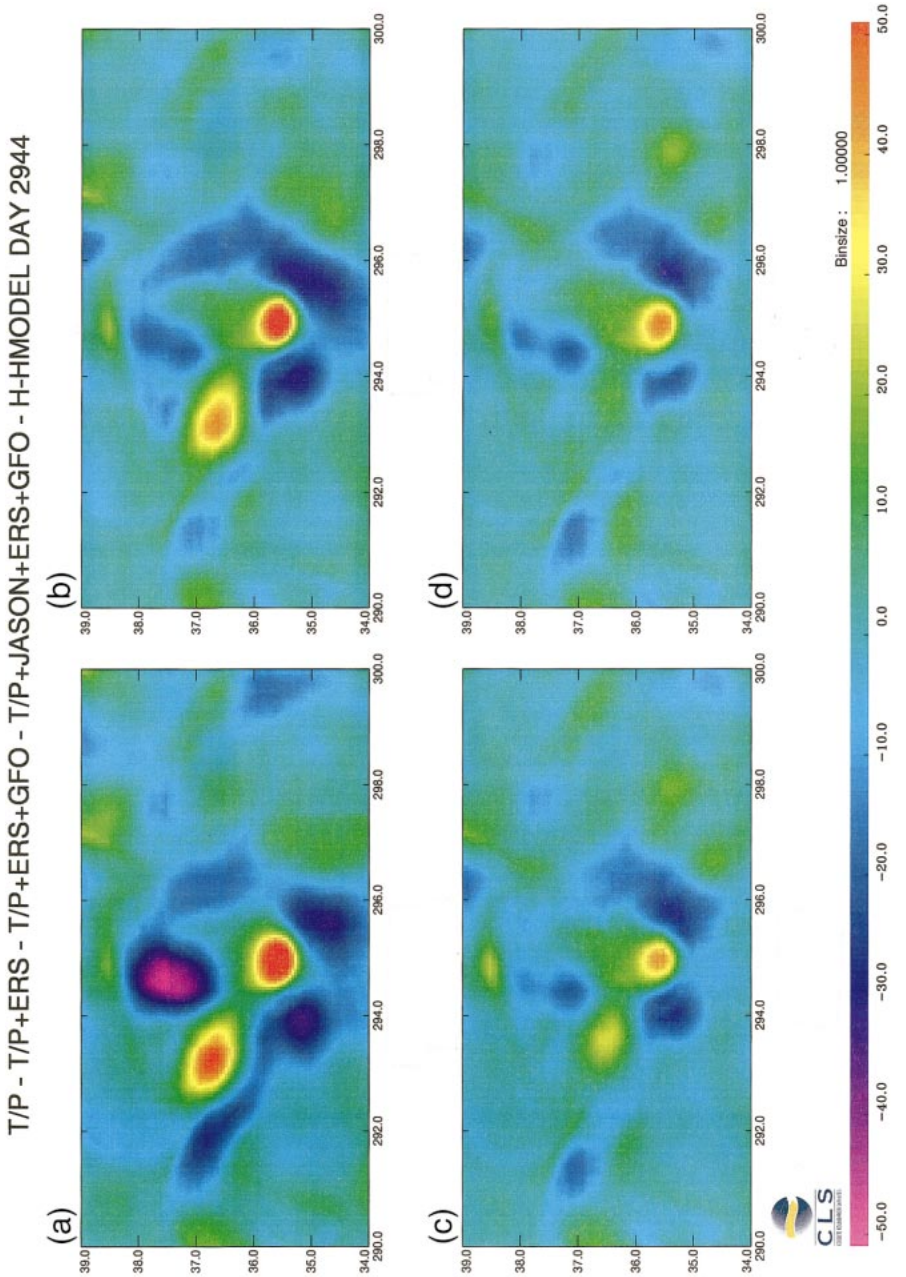

FIG. 3. Sea level mapping error for 23 Jan 1993, i.e., difference between the reference field (Fig. 2b) and the field reconstructed from simulated alongtrack altimeter data for (a) T/P, (b) T/P+ERS, (c) T/P+ERS+GFO, and (d) T/P+Jason-1+ERS+GFO. Units are in centimeters.

1+ERS+GFO, respectively. The rms of the SLA signal is about 37 cm, which means that the relative mapping errors (in percentage of signal variance) are all below 10% except for T/P. However, all the configurations (even the one with four satellites) more or less miss the small time- and space scales of the model. Figure 3 shows that, except for the T/P case, the mapping errors correspond to wavelengths between 100 and 200 km and/or short timescales. In particular, the small cyclonic eddy near 35.5° and 295°E, which has a diameter below 100 km and is associated with propagation velocities larger than 10 km day^{-1} (i.e., with a decorrelation timescale below 5 days), is very poorly reproduced (both in amplitude and position), as well as the rapid evolution of the main meander (associated with a sea level change of about 30 cm in 3 days). If these events are representative of the real ocean, they will be very difficult to map from altimetry (see discussion).

The mapping capability varies in space and time. Some configurations have a mapping error very stable in time (e.g., T/P, T/P+Jason-1), while others have complex space–time variations of mapping errors (GFO, ERS). To complement the previous illustrations, we show the evolution in time of mapping error at a given location for the different satellite configurations (Fig. 4). The point location is situated between two T/P crossovers in the southwest corner of Fig. 2 (34.8°N, 291.5°E). The T/P error is, of course, large (12.8-cm rms). The T/P+ERS error is smaller (10.1-cm rms), while the combination of T/P+Jason-1+ERS+GFO has the smallest error, of course (7.8-cm rms), but the gain relative to the T/P+ERS+GFO configuration is small. The two- and three-satellite combinations have errors generally below ±10 cm and they are much smaller than the signal. Thus, the variations in time of the mapping errors will not be a problem for interpreting the reconstructed ocean signal. These variations are actually more representative of very short time- (and space) scale events in the model fields rather than time inhomogeneity of the mapping error. This is clearly observed near day 300, which corresponds to a very rapid evolution of a Gulf Stream meander (not shown but similar to the one observed in Figs. 2a–d). This type of event is not well captured, even with the four-satellite configuration, because it has time- and space scales of a few days and of a few tens of kilometers, respectively.

4. Statistical results

For each of the analyzed configurations (see section 2), the sea level mapping errors were calculated over one year (1993) over the full domain coverage. Results for T/P, T/P+ERS, T/P+ERS+GFO, and T/P+ERS+Jason-1+GFO are shown in Figs. 5a–d. They can be compared with Fig. 1a, which represents the model rms sea level variability. Figure 6 gives the mean mapping errors in percentage of signal variance, respectively, for the whole North Atlantic (only waters with bathymetry deeper than 500 m) and for four different areas (Gulf Stream, Azores Current, North Atlantic Drift, and the Tropics). Note that the errors in percentage of signal variance were calculated by dividing error variance at each grid point by the local signal variance.

The statistics for the global and for the four different areas show the same tendencies, although differences in time- and space scales of signals somewhat modify the mapping capabilities of the different configurations. There is a clear improvement of mapping capability when going from one to two satellites. Compared to T/P, the T/P+ERS error variance is typically reduced by a factor between 2 and 3. Compared to the T/P+ERS case, the error variance decreases for three and four satellites by 20% to 40% and 40% to 80%, respectively. However, even with the four-satellite configuration, the mapping errors remain everywhere larger than 5% of the signal variance. The Gulf Stream area is the area where the relative contribution of a third and a fourth altimeter is the largest. The gain between an optimized two-satellite configuration (T/P+Jason-1) and a nonoptimized configuration (T/P+ERS) is around 10% except for the Gulf Stream area, where it reaches 30% (see Fig. 6). In this area, the more regular sampling of the T/P+*Jason-1* configuration better captures the high-wavenumber and high-frequency signals (see discussion).

The global area comprises very low eddy energy regions where the dynamics are no more dominated by mesoscale variability. In particular, the high-latitude and shallow regions are characterized by high-frequency signals, which cannot be mapped adequately (see discussion). As a result, the mapping error in percentage of signal variance for the global area is the largest. Low eddy energy regions are also more sensitive to altimeter noise (3-cm rms).

Finally, note that the characterization of the mapping errors in terms of an rms value is somewhat incomplete. As previously mentioned, errors can have large and rapid variations due to particular spatial or temporal events in the model fields. As an illustration, Fig. 7 shows the distribution of mapping errors for the T/P+ERS configuration in the Gulf Stream area. The dotted curve shows the equivalent Gaussian distribution (same standard deviation—same number of data points). The distribution of errors is clearly not Gaussian. Many more data points have errors lower than that for a Gaussian distribution and a few (<1%) data points have larger errors (see also Fig. 4). An rms value is thus probably a pessimistic characterization of the mean mapping error and another norm (e.g., L1) may be better adapted. It nevertheless provides a good means of comparing the different configurations.

5. Discussion

a. Mapping errors and their relation with high-frequency LAM signals

Figure 8 shows the rms of LAM signals with periods shorter than 20 days (estimated from a time spectral anal-

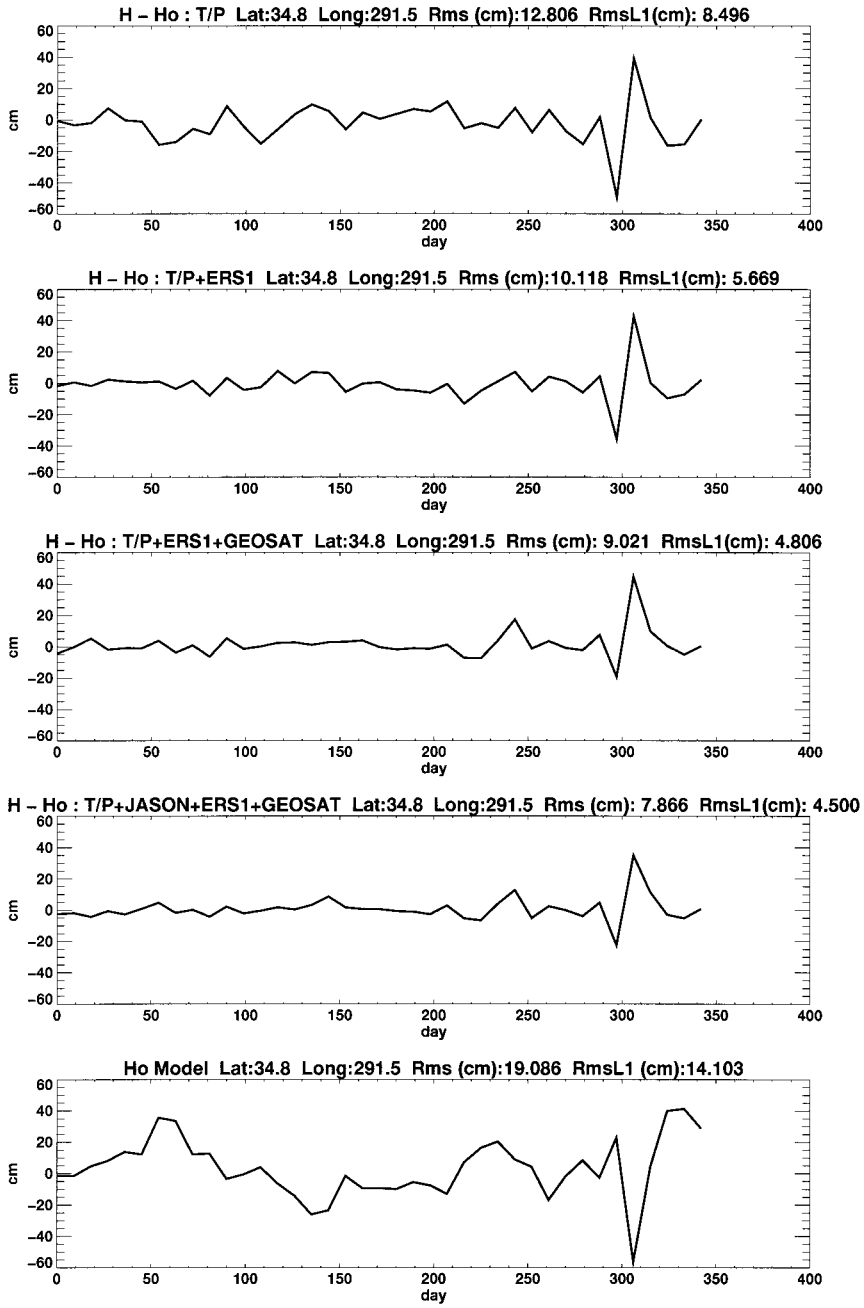

FIG. 4. Evolution in time of the sea level mapping error at 34.8°N, 291.5°E for T/P, T/P+ERS, T/P+ERS+GFO, and T/P+Jason-1+ERS+GFO. Units are in centimeters.

ysis). These high-frequency signals are not resolved even along T/P or *Jason-1* tracks and are thus unlikely to be resolved with the analyzed multiple-altimeter configurations. Figure 9 represents the rms of high-wavenumber LAM signals as estimated from a 2D Loess filter (Schlax and Chelton 1992) with a cutoff wavelength of 2° in latitude and longitude (this is approximately equivalent to a box average over 1.2°; see GSC97). In regions dominated by mesoscale variability, high-frequency signals are mainly associated with high-wavenumber signals (linear dispersion relation). To adequately map these high-frequency and high-wavenumber signals, a time and space resolution better than 10 days and 100 km would be required. This cannot be achieved with any of the analyzed satellite configurations. In regions of low eddy energy at high latitudes and in shallow regions, high-frequency signals are no more associated with high-wavenumber signals. There, high-frequency signals probably mainly correspond to large-scale barotropic signals. These signals are also not adequately mapped with the mapping technique used here and

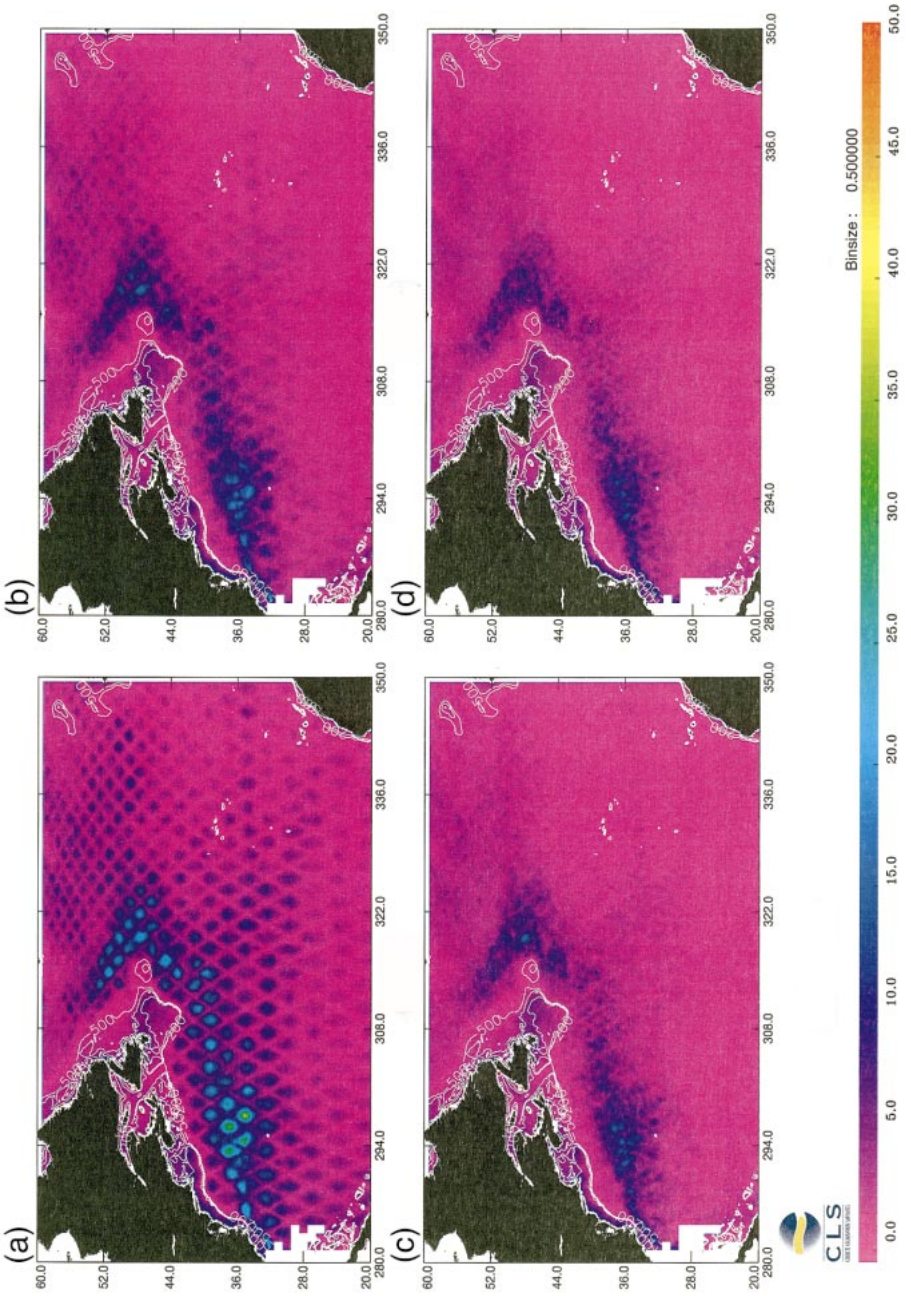

FIG. 5. Rms sea level mapping error for (a) T/P, (b) T/P+ERS, (c) T/P+ERS+GFO, and (d) T/P+Jason-1+ERS+GFO.

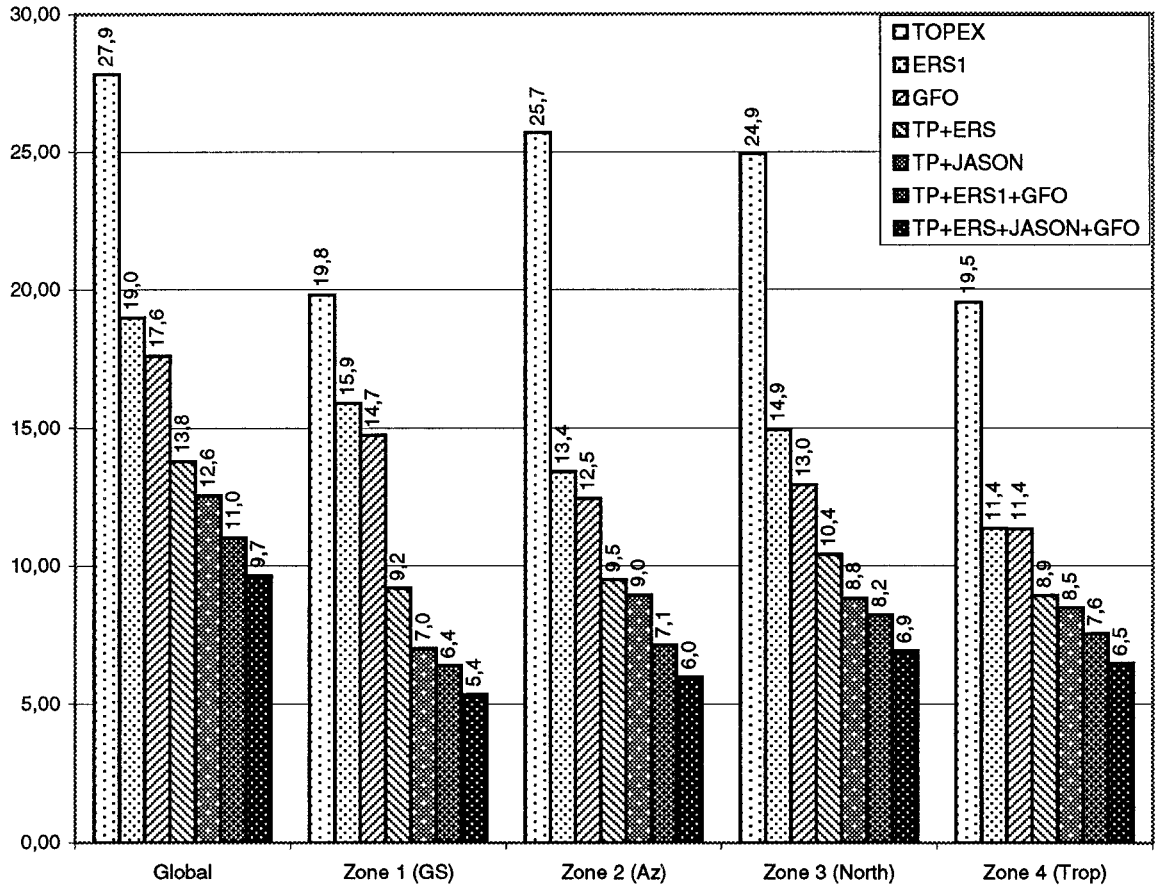

FIG. 6. Mean of the sea level mapping error (in percentage of signal variance) over the whole North Atlantic, the Gulf Stream area (34°–39°N, 70°–60°W), the Azores Current area (32°–36°N, 26°–16°W), the North Atlantic Drift area (45°–55°N, 30°–20°W) and the Tropics area (20°–25°N, 50°–30°W).

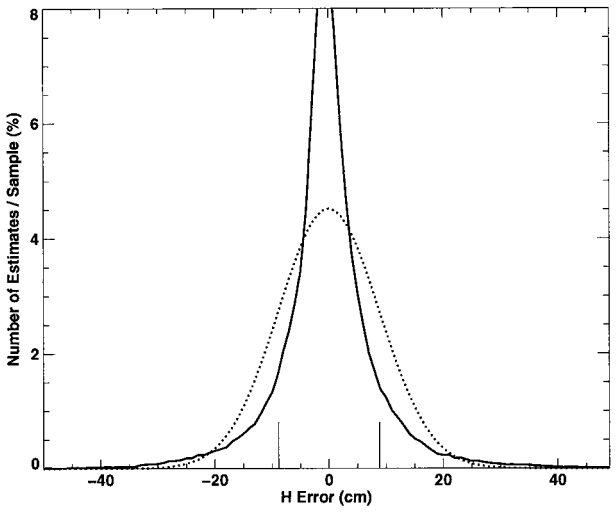

FIG. 7. Distribution of mapping errors for the T/P+ERS configuration in the Gulf Stream area. The dotted curve shows the equivalent Gaussian distribution (same standard deviation, same number of data points).

can be a significant source of aliasing (e.g., Tierney et al. 2000). The mapping technique could be adapted, however, to map these signals and/or to filter them out (Le Traon et al. 1998; Ducet et al. 2000). Since they are of large scale, they can be indeed partly resolved with multiple altimeters (see GSC97).

The high-frequency signals thus clearly limit the mapping accuracy of the analyzed multiple-altimeter configurations and they explain a large part of the mapping errors. This is well illustrated by the close correspondence between the spatial distribution of the mapping error (expressed in percentage of signal variance) for the four-satellite configuration (Fig. 10) and of the relative variance of the high-frequency LAM signals (Fig. 11). In the Gulf Stream area, high-frequency signals have an rms of about 7–10 cm, that is, about 5% of the total signal variance. This is close to the mapping errors shown in Fig. 10. The same holds for other regions dominated by mesoscale variability (e.g., North Atlantic Drift). In regions of low eddy energy at high latitudes and in shallow areas, signals with periods below 20 days generally account for more than 30% of the total signal variance. This is also where mapping errors are larger

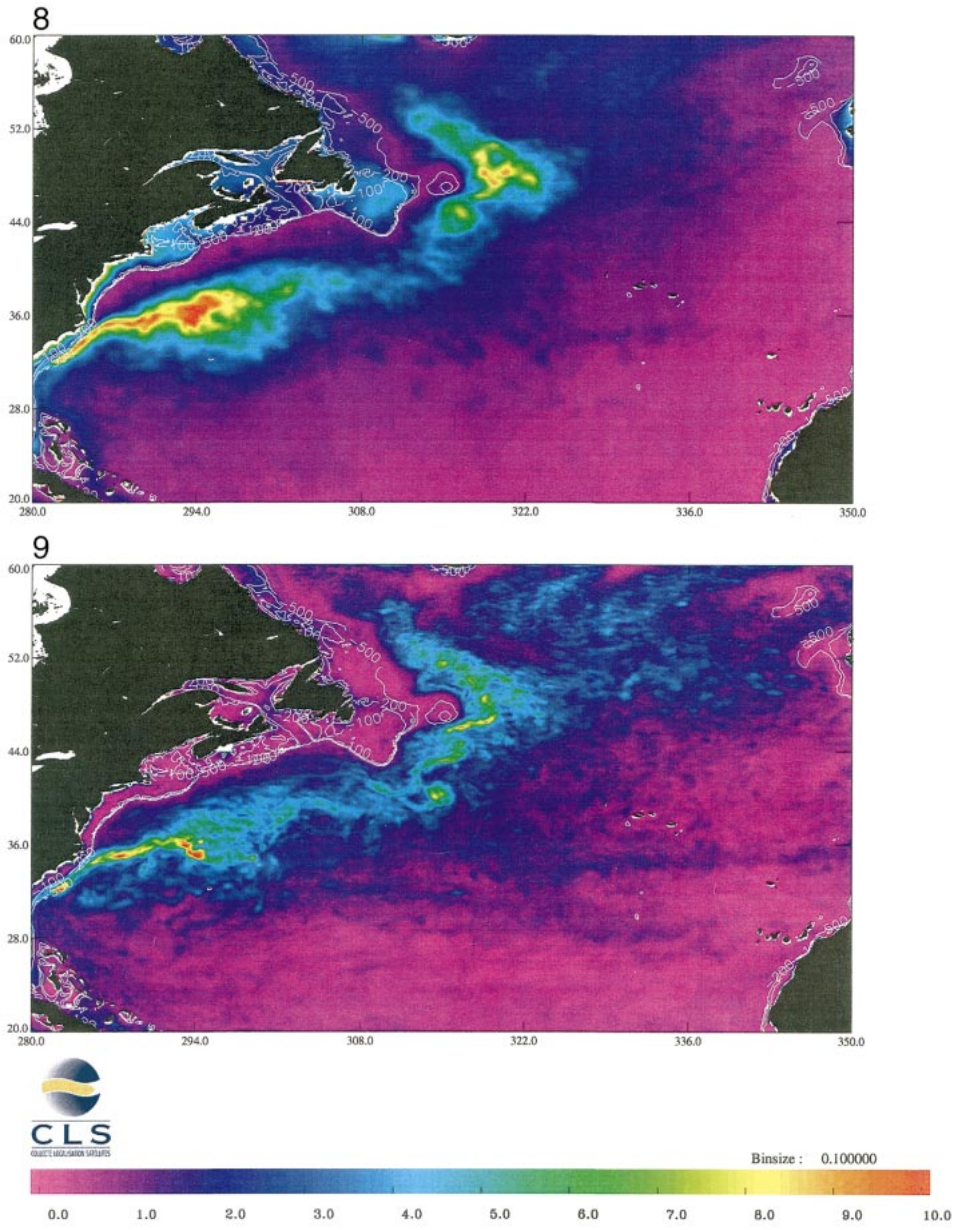

FIG. 8. Rms of LAM signals for periods between 6 and 20 days. Units are in centimeters. FIG. 9. Rms of LAM high-wavenumber signals (Loess filter with a cutoff of 2°). Units are in centimeters.

than 30% of the signal variance. Note, however, that this corresponds to errors of a few centimeters rms only, as the signal is very weak in these regions.

These results also suggest that mapping errors on 10-day average fields will be much smaller than mapping errors on ''instantaneous'' fields as most of the errors (at least for the three- and four-satellite configurations) are due to high-frequency signals.

b. Degree of realism of LAM signals

A central assumption to this analysis is that the model is a realistic representation of the ocean. Smith et al. (2000) have shown that the first-order model statistics (variance) are in good agreement with what we know from altimetry (see also Figs. 1a,b). The repartition of this energy according to wavenumber and frequency is more difficult to test. Ducet (2000) has shown that the model time- and space scales compare well with the ones deduced from altimetry. The main concern (because it has the largest impact in our analysis) is the high-frequency and high-wavenumber spectral content of the model fields. One possible validation of the relative importance of this spectral band can be deduced from the analysis of an *ERS-1* 3-day repeat period. Min-

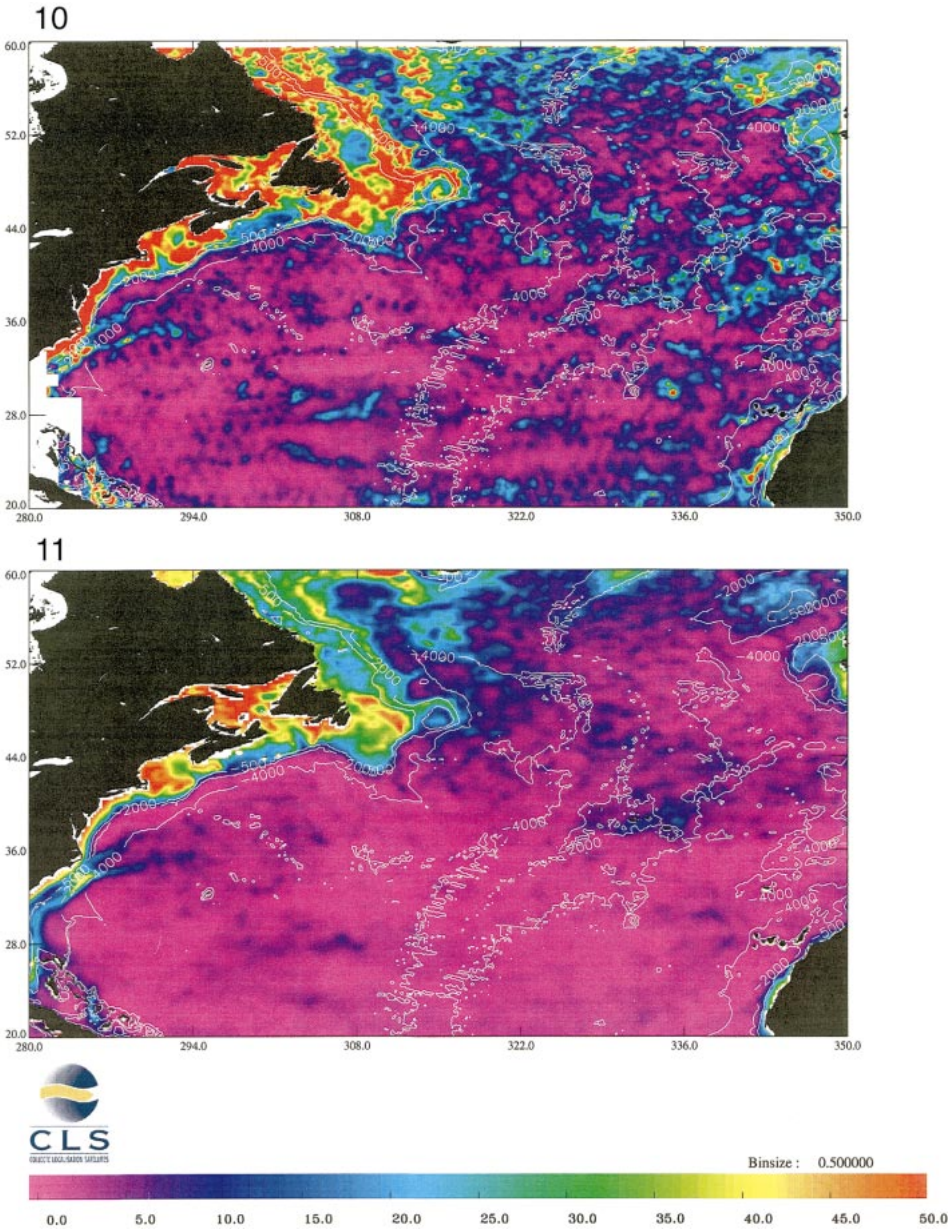

FIG. 10. Mapping error for the analyzed four-satellite configuration (T/P+Jason-1+ERS+GFO) expressed in percentage of signal variance. FIG. 11. Contribution of high-frequency signals (periods between 6 and 20 days) to the total LAM sea level variance. Units are percentage of signal variance. Bathymetric contours for 500, 2000, and 4000 m are superimposed.

ster and Gennero (1995) have shown that in the Gulf Stream less than 5% of the energy is found at periods below 20 days. This is comparable (although slightly smaller) with what we found here in the band 6–20 days. The model thus appears to be rather close to what we know on the frequency/wavenumber spectrum of the ocean. There is a need, however, for a more in-depth validation of the model statistical characteristics, a task that is clearly beyond the scope of this note.

c. Comparison with LD99 results

The mapping errors are also larger than the one derived from LD99 formal error analysis for their reference estimation (ZC = 150 km, ET = 15 days). In particular, their decrease according to the number of altimeters is not as fast. While the one-satellite mapping errors are only slightly larger (except for T/P), the two-, three-, and four-satellite configurations have mapping

errors (in percentage of signal variance) larger by factors of about 1.5, 1.8, and 2, respectively, in the Gulf Stream area. This is probably due to the high-frequency variability of the model, which is not well represented in the LD99 (and ours) simplified covariance model. In particular, the correspondence between small spatial scales and small timescales is not taken into account. In addition, the LD99 (and ours) chosen timescale (15 days) is slightly too large at high latitudes (Ducet 2000). This probably explains why LD99 formal errors may be underestimated.

The mapping errors are also larger than the ones derived from a lower-resolution model [Parallel Ocean Climate Model (POCM)—1/4 of a degree model] by a factor of almost 10 (LD99). This is because POCM (as other intermediate resolution models) has a very low level of mesoscale variability and has too large time- and space scales. As a result, and as already mentioned by LD99, it provides a very optimistic view of the mapping capabilities of the different altimeter configurations.

6. Conclusions

The availability of high-resolution primitive equation models with realistic mesoscale variability has opened up a new scope for analyzing the contribution of single- and multiple-altimeter missions. The study has quantified how well single- and multiple-altimeter missions can map a very complex (and realistic) field of motion where high- and low-frequency and high- and low-wavenumber signals are superimposed. These results confirm the main conclusions of the LD99 study based on formal error analysis. There is, in particular, a large improvement in mapping capability when going from one satellite to two satellites. Mapping errors (in percentage of the signal variance) are, however, larger than the ones derived from LD99 formal error analysis (by a factor between 1.5 and 2). This is mostly due to the LAM high-frequency signals (periods $<$ 20 days). In regions dominated by mesoscale variability, these signals have a variance larger than 5% of the total sea level variance; they are mainly associated with high-wavenumber signals. Such signals cannot be resolved with any of the analyzed multiple-altimeter configurations. As a result, mapping errors always remain larger than 5% of the signal variance and do not decrease as rapidly as expected. In high-latitude low eddy energy regions and in shallow waters, the high-frequency signals have a variance generally larger than 30% of the total sea level variance and the relative mapping errors are also larger than 30%. These (small) signals are, however, associated with larger spatial scales, and mapping techniques could be adapted to better map them.

Thus, while the main time- and space scales of mesoscale variability are reasonably well mapped with existing and future two-satellite configurations, the mapping of the smaller time- and space scales will require a much better resolution (e.g., better than 10 days and 100 km). In particular, the time resolution should be increased to adequately sample the high-frequency signals.

Acknowledgments. We thank R. Smith for providing us with the Los Alamos model outputs. The study was funded by CNES under Contract CNES/CLS 794/99/7805/00.

REFERENCES

Blayo, E., T. Mailly, B. Barnier, P. Brasseur, C. Le Provost, J. M. Molines, and J. Verron, 1997: Complementarity of *ERS-1* and TOPEX/POSEIDON altimeter data in estimating the ocean circulation: assimilation into a model of the North Atlantic. *J. Geophys. Res.,* **102,** 18 573–18 584.

Chassignet, E. P., W. R. Holland, and A. Capotondi, 1992: Impact of the altimeter orbit on the reproduction of oceanic rings: Application to a regional model of the Gulf Stream. *Oceanol. Acta,* **15,** 479–490.

Ducet, N., 2000: Combinaison des données altimétriques TOPEX/Poseidon et ERS-1/2 pour l'étude de la variabilité océanique mésoéchelle. Comparaison avec un modèle à haute résolution de l'océan Atlantique Nord. Ph.D. thesis, Université Paul Sabatier, Toulouse, France, 242 pp.

——, P. Y. Le Traon, and G. Reverdin, 2000: Global high-resolution mapping of the ocean circulation from TOPEX/POSEIDON and *ERS-1/2*. *J. Geophys. Res.,* **105,** 19 477–19 498.

Greenslade, D. J. M., D. B. Chelton, and M. G. Schlax, 1997: The midlatitude resolution capability of sea level fields constructed from single and multiple satellite altimeter datasets. *J. Atmos. Oceanic Technol.,* **14,** 849–870.

Koblinsky, C. J., P. Gaspar, and G. Lagerloef, Eds., 1992: The future of spaceborne altimetry: Oceans and climate change. Tech. Rep., Joint Oceanographic Institutions Incorporated, Washington, DC, 75 pp.

Le Traon, P. Y., and F. Ogor, 1998: *ERS-1/2* orbit improvement using TOPEX/POSEIDON: The 2 cm challenge. *J. Geophys. Res.,* **103,** 8045–8057.

——, and G. Dibarboure, 1999: Mesoscale mapping capabilities from multiple-satellite altimeter missions. *J. Atmos. Oceanic Technol.,* **16,** 1208–1223.

——, F. Nadal, and N. Ducet, 1998: An improved mapping method of multi-satellite altimeter data. *J. Atmos. Oceanic Technol.,* **15,** 522–534.

Minster, J. F., and M. C. Gennero, 1995: High-frequency variability of western boundary currents using *ERS-1* three-day repeat altimeter data. *J. Geophys. Res.,* **100,** 22 603–22 612.

Schlax, M. G., and D. B. Chelton, 1992: Frequency domain diagnostics for linear smoothers. *J. Amer. Stat. Assoc.,* **87,** 1070–1081.

Smith, R. D., M. E. Maltrud, F. O. Bryan, and M. W. Hecht, 2000: Numerical simulation of the North Atlantic Ocean at 1/10°. *J. Phys. Oceanogr.,* **30,** 1532–1561.

Stammer, D., 1997: Global characteristics of ocean variability estimated from regional TOPEX/POSEIDON altimeter measurements. *J. Phys. Oceanogr.,* **27,** 1743–1769.

Tierney, C., J. Wahr, F. Bryan, and V. Zlotnicki, 2000: Short-period oceanic circulation; Implication for satellite altimetry. *Geophys. Res. Lett.,* **27,** 1255–1258.

Wunsch, C., 1989: Sampling characteristics of satellite orbits. *J. Atmos. Oceanic Technol.,* **6,** 892–907.